Journal of Biomolecular Screening
http://jbx.sagepub.com

A Simple, No-Wash Cell Adhesion–Based High-Throughput Assay for the Discovery of Small-Molecule Regulators of the Integrin CD11b/CD18

Jun Y. Park, M. Amin Arnaout and Vineet Gupta

J Biomol Screen 2007; 12; 406
DOI: 10.1177/1087057106299162

The online version of this article can be found at:
http://jbx.sagepub.com/cgi/content/abstract/12/3/406

Published by:
SAGE Publications
http://www.sagepublications.com

On behalf of:
SBS
Society for Biomolecular Sciences

A Simple, No-Wash Cell Adhesion–Based High-Throughput Assay for the Discovery of Small-Molecule Regulators of the Integrin CD11b/CD18

JUN Y. PARK, M. AMIN ARNAOUT, and VINEET GUPTA

The leukocyte-specific integrin CD11b/CD18 plays a key role in the biological function of these cells and represents a validated therapeutic target for inflammatory diseases. Currently, the low affinity interaction between CD11b/CD18 integrin and its respective ligand poses a challenge in the development of cell-based adhesion assays for the high-throughput screening (HTS) environment. Here the authors describe a simple cell-based adhesion assay that can be readily used for HTS for the discovery of functional regulators of CD11b/CD18. The assay consistently produces acceptable Z´ values (> 0.5) for HTS. After testing the assay using 2 established blocking antibodies as reference biologicals, the authors performed a proof-of-concept primary screen using a library of 6612 compounds and identified both agonist and antagonist hits. (*Journal of Biomolecular Screening* 2007:406-417)

Key words: integrin, no-wash assay, cell adhesion assay, primary screen

INTRODUCTION

INTEGRINS ARE NONCOVALENTLY LINKED α/β heterodimeric receptors that mediate cell adhesion, migration, and signaling.[1] Together with their ligands, integrins play central roles in many processes, including development, hemostasis, inflammation, and immunity, and in pathologic conditions such as cancer invasion and cardiovascular disease. The β2 integrins, which have a common β-subunit (β2, CD18) but distinct α-subunits (CD11a, CD11b, CD11c, and CD11d), are critical leukocyte receptors that are important not only for the function of leukocytes but also for the development of the inflammatory response in vivo.[2] Leukocytes normally circulate in the vasculature in a quiescent state but, in response to inflammatory stimuli, adhere, transmigrate across the vascular endothelium, and enter areas of tissue inflammation, where they participate in the destruction and removal of infectious agents and in amplifying the process of inflammation. The integrin CD11b/CD18 (complement receptor type 3 [CR3], Mac-1, or αMβ2) is the predominant β2 integrin receptor in neutrophils, macrophages, and monocytes and mediates a large number of pro-inflammatory functions in these cells.[3,4] CD11b/CD18 recognizes a wide variety of ligands, including the complement fragment iC3b, fibrinogen, blood-clotting factor X, CD54 (ICAM-1), the hookworm neutrophil inhibitory factor (NIF), and denatured proteins such as bovine serum albumin (BSA).[5] Studies in $CD11b^{-/-}$ mice have shown that this integrin has a distinct and cooperative role (with integrin CD11a) in the inflammatory process.[6] In addition to the knockout mice studies, the biological importance of this integrin in maintaining immunological homeostasis has been illustrated by different pathological conditions where integrins are absent or defective—loss of functional β2 integrins causes life-threatening infections in humans, and mutations result in leukocyte adhesion deficiency type 1, where circulating neutrophils fail to adhere to or migrate across the endothelium and the patients are susceptible to recurrent, life-threatening bacterial infections.[7-9] Similarly, improper excessive activation of leukocyte integrins is also harmful, as overactivation of β2 integrins contributes to sustained inflammation, ischemia-reperfusion injury (including acute renal failure, atherosclerosis and autoimmune disorders,[1,7] and tissue damage[10]), and the development of various autoimmune diseases.[11] CD11b/CD18 is also implicated in stroke,[12] neointimal thickening in response to vascular injury,[2] bullous pemphigoid,[13] and neonatal obstructive

Nephrology Division, Leukocyte Biology and Inflammation Program, Massachusetts General Hospital, Harvard Medical School, Charlestown, MA.

Received Aug 31, 2006, and in revised form Nov 3, 2006. Accepted for publication Nov 21, 2006.

Journal of Biomolecular Screening 12(3); 2007
DOI:10.1177/1087057106299162

nephropathy.[14] Thus, there is a considerable potential for agents that block the binding of CD11b/CD18 to its physiologic ligands as therapeutics for the treatment of such inflammatory conditions.

Physiologic ligand binding by CD11b/CD18 is divalent cation dependent and is mediated by CD11b von Willebrand factor type A (VWFA) domain, CD11bA-domain (αA-domain).[15] Blocking anti-CD11b/CD18 antibodies decreases ischemia/reperfusion injury,[16] the area of myocardial infarction,[17] and liver cell injuries,[18] and it diminishes neointimal thickening and restenosis after balloon injury of carotid arteries[19] in animal models. These antibodies are also effective in the treatment of endotoxic challenge and hemorrhagic shock[20] and autoimmune injury in various organs, including the kidney. However, antibody therapy is not ideal, as adverse effects due to nonselective blockade of various other leukocyte functions may lead to severe complications.[21] Similarly, NIF, a 41-kDa glycoprotein ligand mimic, is effective in attenuating the deleterious effects of excessive neutrophil activation in animal models,[22] but its large size and immunogenecity preclude its use as a therapeutic agent. In addition, although blockade of the binding sites of integrins with ligand-mimetic peptides or small molecules has proved effective in inhibiting the activities of β1 and β3 integrins, peptides derived either from CD11b/CD18 ligands or anti-CD11b/CD18 antibodies were not very efficacious in blocking ligand binding in vitro.[23] The failure of these ligand-mimetic peptides to block the interaction between iC3b and CD11b/CD18 may be due to their improper conformation in solution or to the size of the ligand-binding sites, which may be too extensive to block with a small peptide. The identification of small molecules that selectively modulate CD11b/CD18 ligand binding, especially by targeting allosteric regulatory sites, such as the hydrophobic site-for-isoleucine (SILEN) pocket in CD11b/CD18,[24] may prove to be a more promising therapeutic strategy, as has been shown by the discovery of several small-molecule antagonists targeting a similar site for the related integrin CD11a/CD18.[25] Progress is being made in that direction, with 2 recent reports describing identification of a few small molecules targeting CD11b/CD18.[26,27] However, current assays rely on purified proteins adsorbed to microplates, and even though these assays are compatible with high-throughput screening (HTS), purification of the requisite amount of CD11b/CD18 from mammalian cells for the HTS campaign can be exceedingly difficult and may not retain the natural conformation of integrin upon adsorption to the plastic surfaces. Optimized cell-based phenotypic assays that can be readily used in an HTS environment for the rapid identification of small-molecule regulators of this important integrin are currently lacking. Recent reports also suggest that CD11b/CD18 has a central role in the resolution of the inflammatory process, by modulating the egress of adherent neutrophils from the site of inflammation.[28] This suggests that small-molecule agonists of CD11b/CD18 may also have a role in the treatment of certain inflammatory and other conditions. Here again, simple cell-based phenotypic assays for ready HTS adaptation are currently lacking. In this report, we describe a convenient, no-wash cell adhesion–based HTS assay in the 384-well plate format for the discovery of small-molecule regulators of the integrin CD11b/CD18. The adhesion assay does not require expensive reagents, is very quick, and provides a quantitative and consistent readout. In addition, the assay can be used for the identification of either agonists or antagonists of integrin function. In a proof-of-concept study, we used this assay to perform a primary screen using a commercially available library of small molecules to identify ones that would modulate integrin CD11b/CD18-based cell adhesion. A small number of novel compounds were identified as either agonists or antagonists in this primary screen.

MATERIALS AND METHODS

Reagents and antibodies

Restriction and modification enzymes were obtained from New England Biolabs (Beverly, MA), GIBCO BRL (Gaithersburg, MD), or Fisher Scientific (Pittsburgh, PA). Cell culture reagents were from Invitrogen Corp. (San Diego, CA) or Fisher Scientific. The anti-CD11b monoclonal antibody (mAb) 44a (IgG2a),[3] the heterodimer-specific anti-CD18 mAb IB4 (IgG2a),[29] the ligand mimic mAb 107 (IgG1),[30] and an activation-dependent mAb 24 (IgG1)[31] (Abcam, MA) have been described previously. Isotype control antibodies MOPC-21 (IgG1) and MOPC-173 (IgG2a) and FITC-conjugated goat antimouse Ig were from BDPharmingen (San Diego, CA). Human fibrinogen (plasminogen, von Willebrand factor, and fibronectin depleted) was purchased from Enzyme Research Laboratories (South Bend, IN). The 96- and 384-well MaxiSorp microplates were from Nunc (Nalgene, NY), and nonfat milk was purchased from Bio-Rad (Hercules, CA).

Cell culture and stable transfection

Stable transfection of wild-type integrin CD11b/CD18 in K562 cells (ATCC) was performed using published protocols.[32,33] Briefly, K562 cells (K562 mock) were grown to log phase in Iscove's Modified Dulbecco's Medium (IMDM, CellGro), supplemented with 10% heat-inactivated fetal bovine serum and 50 IU/mL penicillin and streptomycin at 37 °C, and resuspended in serum-free IMDM at ~1×10^7/mL. A total of 0.5 mL of cells was transferred into a 0.4-cm cuvette (Fisher), and 10 μg each of linearized wild-type CD11b and wild-type CD18 cDNA pcDNA3 expression vectors carrying a G418-resistance marker[4] was added. Electroporation was carried out at 960 μF and 320 V (Gene-Pulser, Bio-Rad). Transfectants were allowed to recover in serum-containing media for 48 h and were then selected with 0.5 mg/mL G418 (Invitrogen) for up to 2 weeks. CD11b/CD18-expressing cells (K562 wild type) were enriched by fluorescence-activated cell sorting (FACS) using the heterodimer-specific mAb IB4.[32,34] Sorted cells were cloned by limiting dilution, and clones with varying levels of integrin

expression were identified by flow cytometry and maintained in IMDM supplemented with 10% heat-inactivated fetal bovine serum, 50 IU/mL penicillin and streptomycin, and 1 mg/mL G418.

Flow cytometry

Flow cytometric analysis of K562 cells (mock and wild type) was performed using published protocols.[35,36] Briefly, cells were counted and washed twice with phosphate-buffered saline (PBS) containing 1 mM each of Ca^{2+} and Mg^{2+} ions (PBS^{++}). Cells (5×10^5) were incubated with primary mAb (3 μg/mL) in 100 μL PBS^{++} at room temperature for 15 min, except for mAbs 24 and the isotype-matched control mAb MOPC-21, where incubations were performed in Tris-buffered saline (TBS, Boston Bioproducts, Boston, MA) at 37 °C for 30 min and in the presence of either Ca^{2+} and Mg^{2+} (1 mM each) or 1 mM Mn^{2+}[35]. Cells were subsequently washed with PBS^{++} and incubated with FITC-conjugated secondary mAb (5 μg/mL) for 20 min at room temperature. Stained cells were washed and analyzed using the FACS scan flow cytometer (BD Biosciences, San Jose, CA), counting 10,000 events. Data were analyzed using the CellQuest software (BD Biosciences).

Coating microplates with ligand

The 96- and 384-well Maxisorp microplates were coated with 1 to 20 μg/mL fibrinogen (Fg) ligand in PBS^{++} overnight at 4 °C. Subsequently, the Fg-coated wells were washed with TBS, and nonspecific sites were blocked by incubation with 2% nonfat milk in TBS at room temperature for 30 min. Next, the wells were washed 3 times with TBS, and the coated microplates were used in the HTS assays.

HTS adhesion assay

All the adhesion assays were carried out in the screening facility at the Institute of Chemistry and Cell Biology (ICCB), Harvard Medical School, using the available small-molecule libraries and equipment. The Actimol Timtec 1 small-molecule library (6612 compounds) has been previously described (http://iccb.med.harvard.edu/screening/compound_libraries). The small-molecule library is stocked in 384-well plates at –80 °C and as sealed plates, with each well containing a unique compound dissolved in DMSO at approximately 5 mg/mL. For the adhesion assay, the K562 cells were washed with TBS, and cells (50,000/well for 96-well plates and 20,000/well for 384-well plates) were transferred to the Fg-coated wells of microplates in the assay buffer (TBS containing 1 mM each of Ca^{2+} and Mg^{2+} [TBS^{++}] for agonist identification assays or TBS for antagonist identification assays). Compounds were transferred to each well using a pin-transfer robot (Seiko D-TRAN XM3106-31 PN 4-axis Cartesian robot) with a 384-transfer pin (V&P Scientific, San Diego, CA) calibrated at 100 nL, and the assay plates were incubated at 37 °C in the presence of small-molecule compounds. In the screen for agonists, the cells were in TBS^{++} and were incubated with small molecules for 30 min. In the screen for antagonists, following incubation of the cells in TBS with small molecules for 20 min at 37 °C, 1 mM Mn^{2+} was added to each well, and the cells were further incubated for an additional 15 min at 37 °C. To dislodge the nonadherent cell, the assay plates were gently inverted and kept in the inverted position for 20 min at room temperature. Adherent cells were quantitated using either cell viability measuring reagents or automated imaging (see below).

Quantitation of adherent cells

For quantitation of adherent cells using a cell viability measuring kit (such as methanethiosulfonate [MTS]–based CellTiter-One [Promega, Madison, WI], CyQuant [Molecular Probes, Carlsbad, CA], or luciferase-based CellTiter-Glo [Promega]), the nonadherent cells were removed by complete aspiration using an automated liquid-handling machine (ELx405, Bio-Tek Instruments, Winooski, VT), and the assay reagent was added according to the manufacturer's instructions. For automated imaging-based quantitation of adherent cells, the nonadherent cells were fixed by adding a small volume of formaldehyde (1.1% v/v final concentration), and the plates were kept inverted for an additional 1 h. Upon cell fixation, the wells were washed with TBS using an automated liquid-handling machine (ELx405), and the adherent cells were fluorescently labeled with DAPI (0.5 μM final in TBS with 0.1% Triton X-100) and quantitated using an automated microscope (see below).

Automated imaging and analysis

A CellWorx automated microscope (Cellomics, Pittsburgh, PA) was set at a 0.3-s exposure using the DAPI filter set to capture 1 to 3 images per well. Digitized photomicrographs were then analyzed using MetaXpress image analysis software (Molecular Devices, Sunnyvale, CA) using the built-in cell count module to quantify nuclear staining. Data output files were analyzed using MS Excel.

Calculation of assay values and hit identification

Using the number of non-small-molecule-treated cells adherent in the basal physiologic buffer condition (1 mM each of Ca^{2+} and Mg^{2+}) as a minimum threshold, any small molecule resulting in > 10-fold increase in cell adhesion was scored as a positive agonist hit. In addition, using the number of non-small-molecule-treated cells adherent in the activating buffer condition (1 mM Mn^{2+}) as a maximum, any small molecule resulting in a 50% to 70% decrease in cell adhesion was scored as a positive antagonist hit.

Statistical analysis and curve fitting

Regression lines were plotted using XLfit4 (ID Business Solutions, Burlington, MA), and EC_{50} and IC_{50} values were calculated using GraphPad Prism (San Diego, CA) with 4-parameter logistic curve fitting, $y = min + (max - min)/(1 + 10^{(logEC50 - x) hillslope})$. All data are reported as mean ± SEM. The Z´ factor was calculated as previously described.[37]

RESULTS AND DISCUSSION

Expression of heterodimeric CD11b/CD18 on K562 cell surface

We chose the erythroleukemic K562 cells for the adhesion assay, as these cells express integrins, native or recombinant, in a default low-affinity state similar to normal leukocytes, and as with leukocytes, the expressed integrins can be activated and made ligand competent by various external stimuli. Thus, these cells provide an excellent context for the discovery of small-molecule regulators of integrin function.[38] We transfected the K562 cells, which do not endogenously express the integrin CD11b/CD18, with wild-type CD11b/CD18 using electroporation and obtained several single-cell clones stably expressing the integrin CD11b/CD18 on the cell surface by FACS sorting using heterodimer-specific mAb IB4,[9] as has been previously described.[33,39] Unlike previous publications, we also obtained and characterized several different clones displaying varying levels of CD11b/CD18 surface expression (**Fig. 1A**), as these clones would be useful in the future for performing dose-response curves to study the dependence of integrin density on the effect of various small-molecule compounds identified from this screen. One clone, designated 3F9, was selected for all the studies presented in this article, and the CD11b/CD18 surface expression level on 3F9 was further characterized with anti-CD11b mAb 44a[3] and with a ligand-mimetic mAb 107,[30] both of which showed binding comparable to that observed with the mAb IB4 (**Fig. 1B**).

The K562 cell surface–expressed integrin CD11b/CD18 is functionally active

K562 cells express wild-type integrin in a largely inactive state,[38] which can be activated by inside-out signals primarily through a change in integrin affinity rather than avidity.[40] We verified that the integrin CD11b/CD18 was expressed in the correct conformational state on the surface of K562 cells using an activation-sensitive mAb, mAb 24, and using CD11b/CD18 physiologic ligand fibrinogen. The mAb 24 binds to an activation- and cation-dependent epitope in the βA and has been widely used as a reporter of the high-affinity state in β2 integrins.[31] We assessed the binding of mAb 24 to CD11b/CD18 expressed on K562 cells using flow cytometry (**Fig. 1C**). Very little binding was seen in the low-affinity integrin conformation in physiologic Ca^{2+} and Mg^{2+} (1 mM each) buffer, which reproducibly increased upon activation with 1 mM Mn^{2+} (**Fig. 1C**), comparable in magnitude to that observed previously in maximally activated β2 integrins expressed in K562 cells,[39] indicating that the integrins become functionally active in the presence of 1 mM Mn^{2+}.

Adhesion of integrin-expressing cells to ligand-coated plates is a classic assay for the study of integrin function and has been used for the study of numerous integrins, ligands, and cell types. Next, we analyzed binding of K562 cells to the physiologic CD11b/CD18 ligand fibrinogen (Fg) using 96-well plates. Fg is a symmetric dimer that is recognized by a number of different integrins and has been shown to be a critical CD11b/CD18 ligand for inflammatory response and host clearance of microbes.[41] Thus, Fg-CD11b/CD18 interaction is an important target for anti- and pro-inflammatory therapeutic strategies. Enzyme-linked immunosorbent assay (ELISA)–based analysis of Fg-coated wells with anti-Fg mAb showed that the ligand coating of the assay plates was highly even and reproducible and displayed very low variability (not shown). K562 cells (50,000/well) in TBS were added to Fg-coated wells of a 96-well plate, in the presence of EDTA (10 mM), Ca^{2+} and Mg^{2+} (1 mM each), or Mn^{2+} (1 mM), and briefly centrifuged at 500 rpm for 10 s. After incubation at 37 °C for 30 min, unbound cells were removed by gentle hand washing, and the adherent cells were quantitated using CellTiter-Glo (Promega). In this system, no Fg binding by CD11b/CD18-expressing cells was observed in the presence of EDTA or the physiologic divalent cations Ca^{2+} and Mg^{2+} (**Fig. 1D**). Activation with 1 mM Mn^{2+} induced a large increase in Fg binding by the CD11b/CD18-expressing cells (**Fig. 1D**), indicating that the adhesion to Fg was CD11b/CD18 dependent.

Adaptation of cell adhesion assay to a 384-well format

Next, the 96-well adhesion assay was directly adapted to the 384-well plate format. The assay was performed as described for the 96-well plate assay (above), except that fewer K562 cells (20,000/well) were used and that the final washing step was carried out using an automated plate washer. Although we did not find any Fg binding by CD11b/CD18-expressing cells in the absence of activating Mn^{2+} ions and that activation with 1 mM Mn^{2+} induced a large increase in Fg binding by the CD11b/CD18-expressing cells (**Fig. 2A**), we were unable to obtain Z´ values ≥ 0.5, despite our every effort to perform the plate washing as gently as possible. In fact, we obtained negative Z´ values from most of our assays, suggesting that this protocol presented high variability and was not compatible with the HTS environment. Examination of the bottom of 384-well plates for visualization of 1-mM Mn^{2+}-treated adherent cells using DAPI staining and photomicrography with an automated microscope (see Materials and Methods) revealed that an uneven

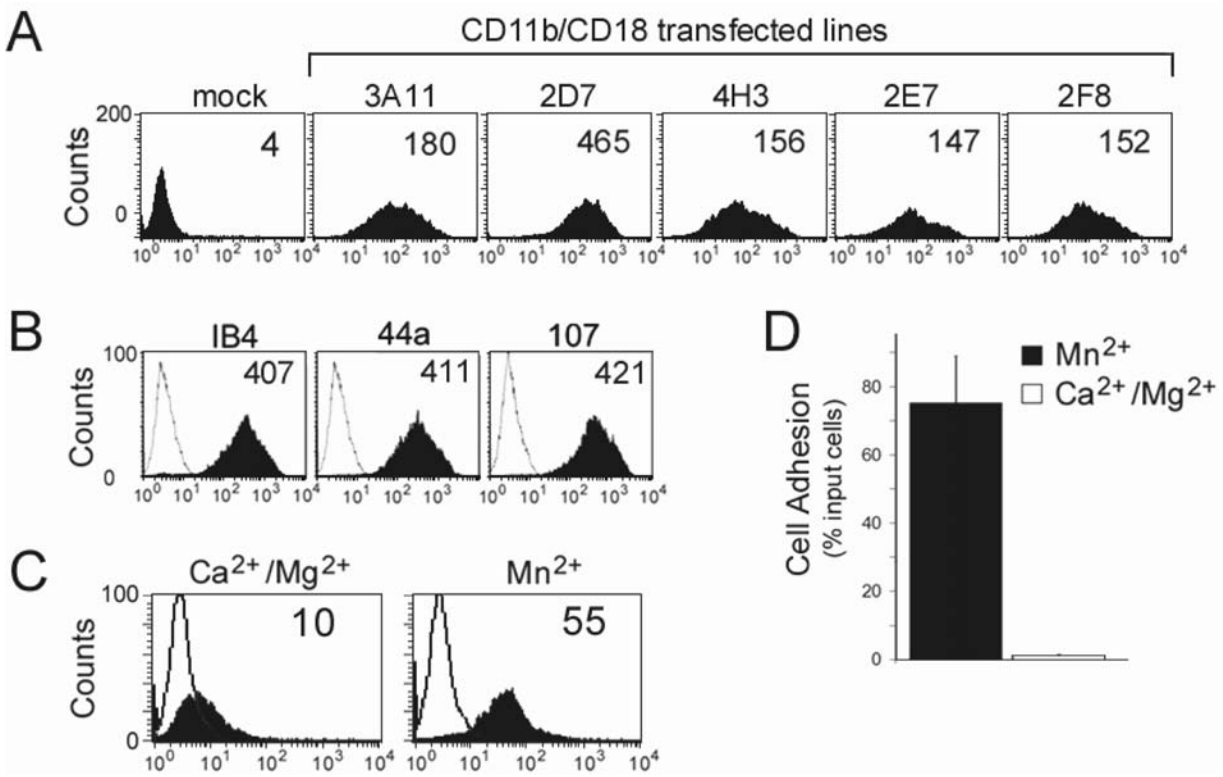

FIG. 1. Characterization of various $CD11b^+/CD18^+$ K562 clones. (**A**) Surface expression profiling of various stable lines generated that express different levels of wild-type CD11b/CD18. FACS histograms showing cells stained with the heterodimer-specific mAb IB4. Mean fluorescence intensity (MFI) for mAb IB4 staining is shown in each panel. IB4 staining of nontransfected cells (mock) was similar to isotype-matched control mAb MOPC-173 (not shown). (**B**) Surface expression profiling of 1 clone (3F9) expressing wild-type CD11b/CD18 at high levels using 3 different mAbs. The MFI for mAb staining is shown in each panel. mAb staining of nontransfected cells (mock) was similar to the isotype-matched control mAb MOPC-173 (not shown). (**C**) Fluorescence-activated cell sorting (FACS) analysis of the reactivity of conformation-sensitive mAb 24. Surface-expressed CD11b/CD18 undergoes activation-dependent conformational change, as measured by mAb 24 binding. K562 cells were incubated with mAb 24 in Tris-buffered saline (TBS) buffer containing Ca^{2+} and Mg^{2+} (1 mM of each) or 1 mM Mn^{2+} at 37 °C, as described.[35] After washing with TBS, cells were stained with FITC-goat antimouse Ig and analyzed, counting 10,000 events. MFI values for mAb staining (filled histogram) are shown in each panel. No binding was observed with isotype control mAb (nonfilled histogram). (**D**) A bar graph showing the percent input cells (50,000 per well) adhering to the bottom of fibrinogen-coated wells in the presence of Ca^{2+} and Mg^{2+} (1 mM of each) or of 1 mM Mn^{2+} and quantitated by the measurement of cellular adenosine triphosphate (ATP) levels from a 96-well plate adhesion assay performed using manual washing of the plate. Each bar represents mean ± SD of triplicate determinations from a representative experiment.

number of cells remained adherent upon completion of the assay, and sometimes cells were completely absent from the middle of the wells (**Fig. 2B**). Upon carefully monitoring the adherent cells in the wells after each step in the assay, we discovered that the automated washing step caused substantial and uneven detachment of adherent cells from wells. Therefore, we reasoned that if one were to identify a gentler way of removing nonadherent cells from the ligand-coated surface of the wells, without necessarily washing the wells, then that would be a way to generate an HTS-compatible assay. Gently inverting the plates and keeping them inverted for a short time provided us with such a methodology. For the complete removal of nonadherent cells prior to quantitation of adherent cells, we developed 2 methods, both of which gave very similar results. In the first method, 1.1% formaldehyde was added, and the adherent cells were fixed to the bottom of 384-well plates, in the inverted position, for 1 h at room temperature. The wells were subsequently washed using an automated plate washer, and the fixed cells were stained with DAPI. DAPI-stained cells were photomicrographed using an automated microscope, and the images of stained nuclei were quantitated using MetaXpress following the manufacturer's recommendations. In the second method, after keeping the plates inverted for a short time, the supernatant containing nonadherent cells was completely aspirated using an automated plate washer, and a developer reagent, such as MTS (which showed the linear dynamic range > 2 logs [not shown]), was added to quantitate cell number. The plates were developed according to the manufacturer's recommendations.

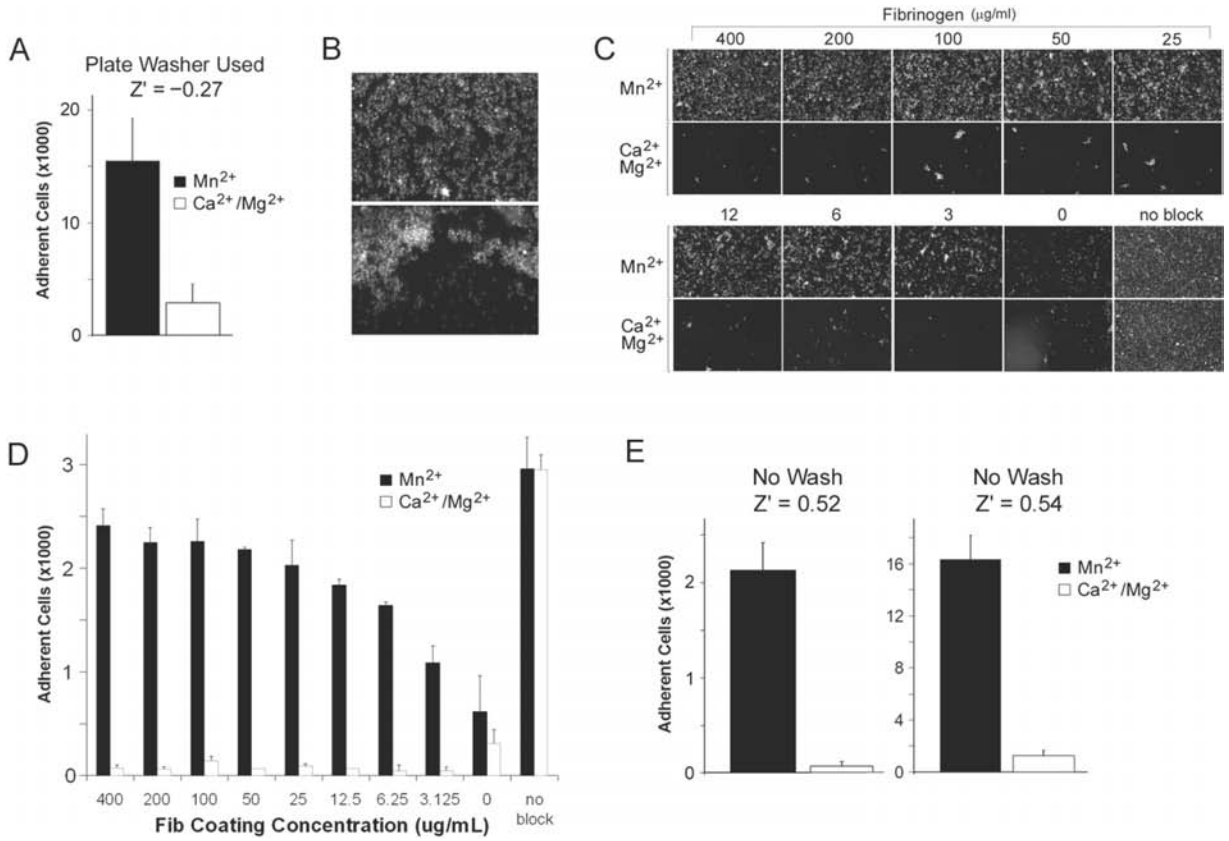

FIG. 2. High-throughput screening (HTS)–compatible no-wash cell adhesion assay in 384-well format. (**A**) A bar graph showing the number of cells adhering to the bottom of fibrinogen-coated wells in the presence of Ca^{2+} and Mg^{2+} (1 mM of each) or of 1 mM Mn^{2+} and quantitated by measurement of cellular adenosine triphosphate (ATP) levels from a 384-well plate adhesion assay performed using automated washing of the plate. Each bar represents mean ± SD of triplicate determinations from a representative experiment. The Z´ values are as indicated. Notice that the automated washing produces a negative Z´ value, rendering the assay unsuitable for HTS applications. (**B**) Example photomicrographs from a 384-well plate adhesion assay showing cells remaining adherent, in the presence of 1 mM Mn^{2+}, before (upper panel) and after (lower panel) automated plate washing. The images clearly show that automated washing, using even the most gentle wash setting, caused substantial and uneven detachment of adherent cells from wells. (**C**) Example photomicrographs from a 384-well plate assay showing cells remaining adherent upon completion of the no-wash cell adhesion assay. Cells were transferred to wells coated with an increasing amount of Fg and incubated in buffer containing either Ca^{2+} and Mg^{2+} (1 mM of each) or 1 mM Mn^{2+} for 20 min at 37 °C. Nonadherent cells were allowed to detach by gentle inversion of the plates, and the adherent cells were fixed with 1.1% formaldehyde. After washing the plate with the automated plate washer and staining cells with DAPI, cells were imaged using an automated microscope. The amount of Fg used to coat the wells is indicated. Cell adhesion to the uncoated well surface is shown (no block). Notice the lack of uneven cell detachment, as seen in **Figure 2B**. (**D**) Bar graphs showing the number of adherent cells as a function of Fg coating concentration. Each bar represents mean ± SD of triplicate determinations from a representative experiment. An automated microscope coupled with image analysis software was used to quantify the adherent cells. (**E**) Bar graphs showing analysis of the assay variability in the no-wash 384-well assay, as measured by quantitation of the adherent cells using an automated microscope (left panel) or methanethiosulfonate (MTS) assay (right panel). Each bar represents mean ± SD across 192 wells from a representative experiment. Cell numbers obtained using the automated microscope are lower than those obtained using MTS, as only ~1/6th of each 384-well was photomicrographed by automated microscope, as compared to the entire well used in the MTS measurement. In both types of analyses, the Z´ value is ≥ 0.5.

Figure 2C shows example photomicrographs from a 384-well plate showing cells adherent to an increasing amount of Fg. These photomicrographs show very little Fg binding by CD11b/CD18-expressing cells in the absence of Mn^{2+} and a large increase in binding upon incubation with Mn^{2+} at every Fg coating concentration tested. Input cell number was estimated by determining cell adhesion to the non-Fg-coated microtiter well surface, which showed high nonspecific binding (**Fig. 2C**, no block). The photomicrographs from triplicate measurements were quantitated using MetaXpress, and the results show that the Fg binding by CD11b/CD18-expressing cells was completely dependent upon activating Mn^{2+} ions and that the variability

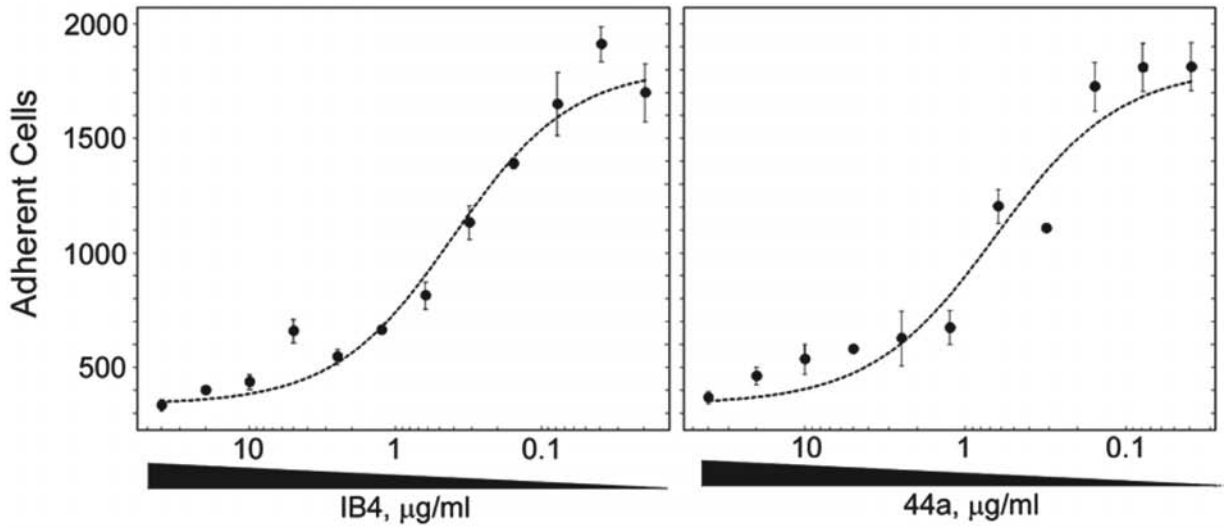

FIG. 3. Dose-dependent inhibition of cell adhesion by blocking mAbs. Shown are dose-response curves depicting number of adherent cells in the presence of an increasing amount of blocking mAbs (IB4, left panel; 44a, right panel). Concentration of mAb used is indicated at the bottom. Curve fitting was done using XLfit4 to show a dose-dependent inhibition of cell adhesion in the presence of 1 mM Mn^{2+}. Each dot represents mean ± SEM of triplicate determinations from a representative experiment.

associated with this assay was very low (**Fig. 2D**). Similarly, binding by CD11b/CD18-expressing cells to a second physiologic ligand iC3b[3] showed high selectivity and low variability (not shown).

Next, we measured the Z´ values across an entire 384-well plate to determine if the optimized assay was ready for an HTS campaign. **Figure 2E** shows that the Z´ values after completion of the adhesion assay were ≥ 0.5 independent of the method used to quantitate the adherent cell number. Although only ~1/6th of each 384 well was photomicrographed using an automated microscope (to keep the imaging and image analysis time to a minimum), whereas the entire well was quantitated using MTS, the Z´ values obtained were very similar to the 2 readouts, suggesting that this simple protocol presented low variability and high compatibility with the HTS environment.

The specificity of CD11b/CD18-expressing cells toward Fg in this assay format was further confirmed by incubation with anti-CD11b (44a[3]) or anti-CD18 (IB4[29]) blocking mAbs. CD11b/CD18-expressing cells were pretreated with an increasing amount of the blocking mAbs for 15 min at room temperature and then allowed to adhere to Fg-coated wells in the presence of Mn^{2+} (1 mM). After incubation at 37 °C for 30 min, unbound cells were removed and the remaining cells were quantitated using automated microscopy, which showed a dose-dependent inhibition of cell adhesion to Fg (**Fig. 3**). Both mAbs produced an IC_{50} value of ~0.5 µg/mL (~3.3 nM), which is similar to the published value (2 nM) for mAb 44a.[26] In addition, very little binding was seen with nontransfected K562 cells under any condition (not shown).

Application of the HTS adhesion assay for identification of novel small-molecule agonists and antagonists

We used the simple, no-wash cell adhesion assay to perform a pilot primary screen to identify small-molecule agonists and antagonists using a library of ~6600 compounds (Actimol Timtec1). In the assay for identifying agonists that produce increased cell adhesion, the cells were transferred to ligand-coated wells of a 384-well plate in TBS buffer containing 1 mM each of Ca^{2+} and Mg^{2+} (TBS^{++}), and compounds were added to each well using a 384 pin-transfer robot. After incubation of the assay plate for 30 min at 37 °C, the nonadherent cells were removed by plate inversion, and the cell number in each well was quantitated using automated microscopy and image analysis. Of the compounds, 144 (2.2%) showed large activation and an increase in cell adhesion (> 10-fold increase over adhesion by nontreated cells). Notably, 21 of the identified compounds had a common substructure to compounds recently identified as CD11b/CD18 agonists in an independent screen using the purified CD11b A-domain[27] (**Fig. 4**). In addition, 1 compound, structurally very similar to RPC-3, was shown to decrease inflammation-induced neutrophil emigration in vivo in thioglycolate-induced peritonitis in mice.[27] This finding that some of the compounds identified in our cell-based screen have a very similar structure to the compounds identified in a purified protein-based screen suggests that at least some of the agonists identified in our phenotypic screen might be acting at the target protein level and not indirectly, through other proteins in the cell. **Figure 5** shows data on 3 of the compounds that showed high

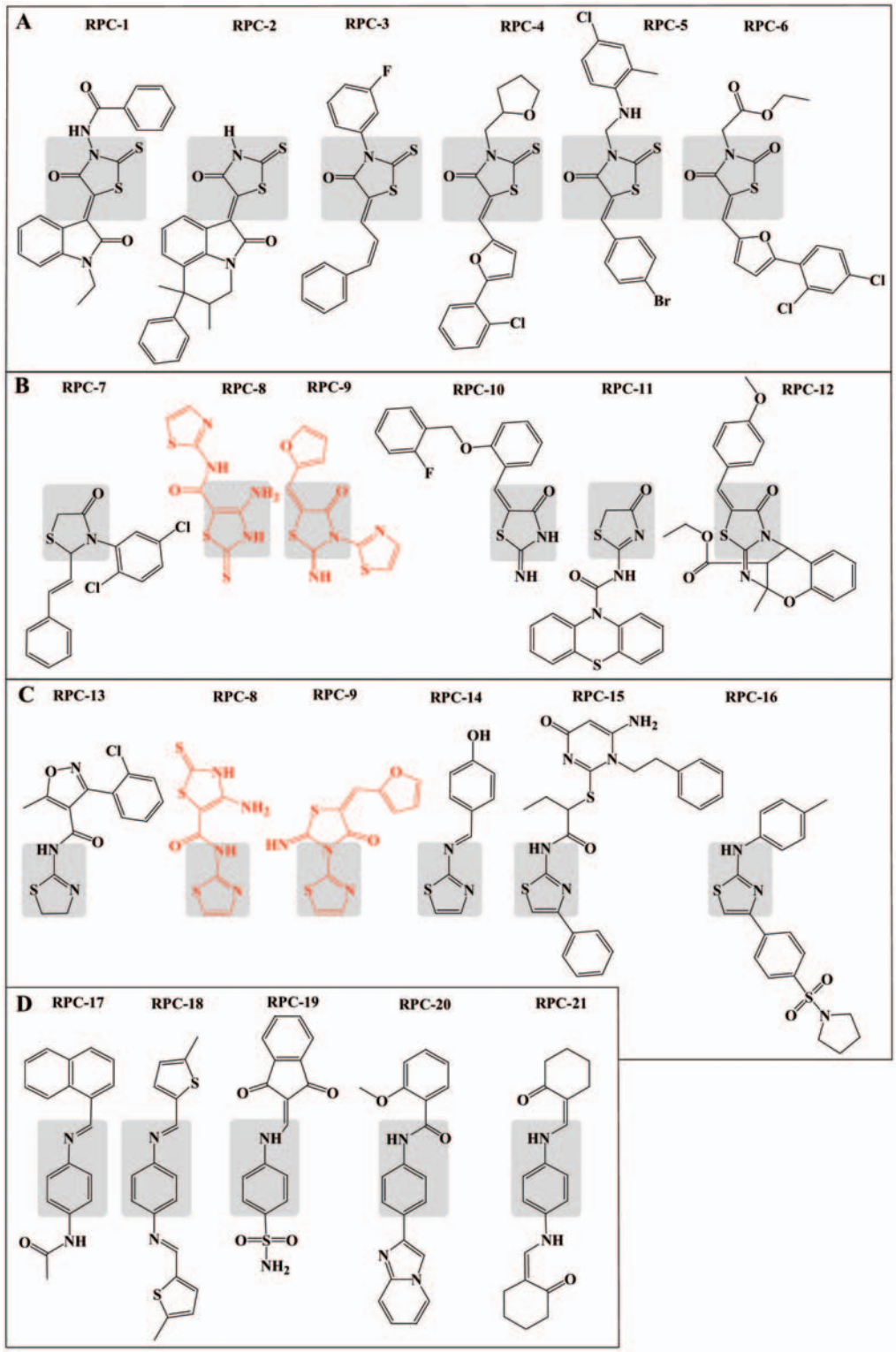

FIG. 4. Structures of a subset of agonists identified in the primary screen. Chemical structures of 21 agonists are shown that are found to contain a substructure similar to compounds recently identified as CD11b/CD18 agonists in a recent study using purified protein.[27] The compounds are categorized in 4 groups (**A**-**D**), similar to the grouping by Bjorklund et al.,[27] of chemically related molecules by visual inspection of the structures (common substructures are highlighted in gray). Two compounds (highlighted in red) have common substructure between the 2 groups.

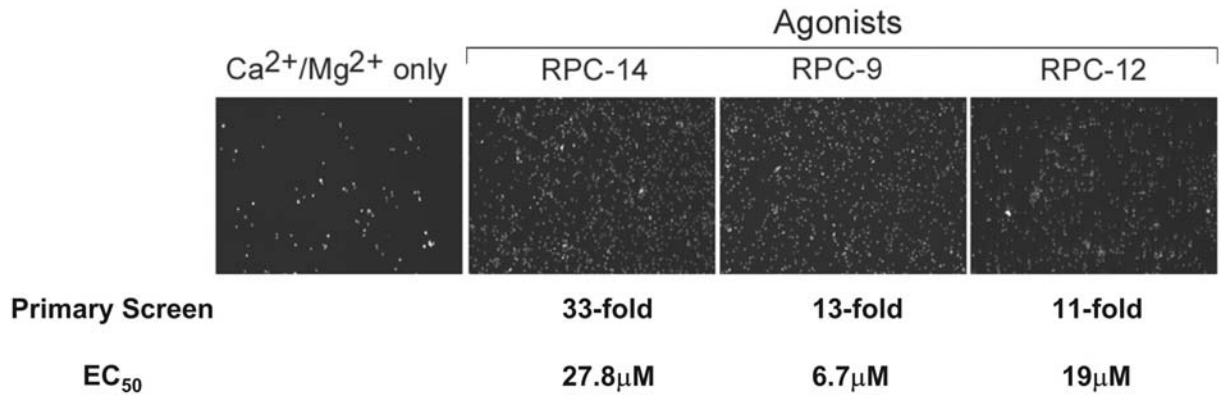

FIG . 5. Primary and secondary screening data for selected agonists. Photomicrographs from the primary screen show increased cell adhesion caused by treatment with 3 of the identified agonists in the physiological buffer condition. Very little cell adhesion is seen in the buffer alone (first panel). The fold increase in the number of adherent cells (over Ca^{2+} + Mg^{2+} levels) in the presence of the indicated compounds is shown under each panel. The EC_{50} value for each of the compounds obtained from the secondary screen is also indicated.

potency in the primary screen (> 10-fold increase in cell adhesion). Next, based on structural uniqueness, we selected 31 compounds from the initial list of 144 for verification in secondary assays. We found that 28 of these cherry-picked compounds were confirmed agonists (although 4 compounds showed a modest 2-fold increase over the background and are thus weak agonists), whereas 3 compounds (RPC-1, RPC-10, and RPC-15) showed no effect, producing a hit confirmation rate of approximately 90%. The hit confirmation rate is unusually high for a primary screen and suggests that, despite using a simple, no-wash protocol, the newly developed assay has high sensitivity. In addition, determination of the concentration required for a half-maximal increase in cell adhesion (EC_{50}) for the 3 selected agonists showed that even though they displayed similar potency in the primary screen, RPC-9 was the most potent of all, with a calculated EC50 value of about 6.7 μM (**Fig. 5**), which is similar to other recently identified agonists.[27] We are currently pursuing the selected leads in additional assays to identify their binding site on the integrin CD11b/CD18.

We further used this assay to identify inhibitors of cell adhesion (antagonists), as described in Materials and Methods. Nonadherent cells were removed, and the cell number in each well was quantitated using MTS. Of the compounds, 22 (0.3%) showed significant (50%-70% decrease) and reproducible (duplicate wells) inhibition (**Fig. 6**). **Figure 7** shows data on 3 of the compounds that showed high potency in the primary screen. **Figure 6** also shows that the identified compounds can be divided into 3 broad groups, based on the presence of common substructures (highlighted in gray), as determined by the visual inspection of the chemical structures. The identified compounds contain a common planar aromatic substructure, reminiscent of the small-molecule inhibitors of the CD11a A-domain that occupy the allosteric SILEN pocket (named IDAS in CD11a).[24,42] Next, we evaluated the 22 compounds in secondary assays. We found that 9 of the selected compounds (RPC-22, RPC-23, RPC-24, RPC-25, RPC-27, RPC-31, RPC-36, RPC-38, and RPC-41, 6 of which are from a single substructure group) showed more than 50% inhibition of cell adhesion and were confirmed antagonists, whereas 8 compounds showed no effect. In addition, the secondary assays were inconclusive for 5 compounds, producing a hit confirmation rate of approximately 53% for antagonists. We further characterized the 3 selected antagonists in secondary assays for determining the concentration needed for 50% inhibition of cell adhesion (IC50), which showed that all 3 were highly potent and had very similar IC50 values (**Fig. 7**). We are currently studying these compounds to determine if they also bind to the allosteric SILEN pocket in the integrin CD11b/CD18. Note that the hit confirmation rate obtained for antagonists in this study is much smaller than the high rate obtained for agonists and could be artificially low due to the small number of compounds studied in the secondary assays. Screening a much larger library of chemical compounds, as we are planning to do in the future, would be needed to determine this number with higher accuracy.

In conclusion, we have developed a simple, no-wash cell adhesion–based assay for HTS of agonists as well as antagonists of the integrin CD11b/CD18. The assay is fast, inexpensive, and easy to implement in an HTS environment. A primary screen with a library of small molecules has identified a number of interesting agonists and antagonists, which are currently being validated in secondary assays. Given the central role of CD11b/CD18 in regulating leukocyte function, we believe that the identification of novel regulators of this integrin not only will provide lead compounds as potential therapeutics but also will generate important new chemical biology tools for the study of the mechanism of integrin activation and function.

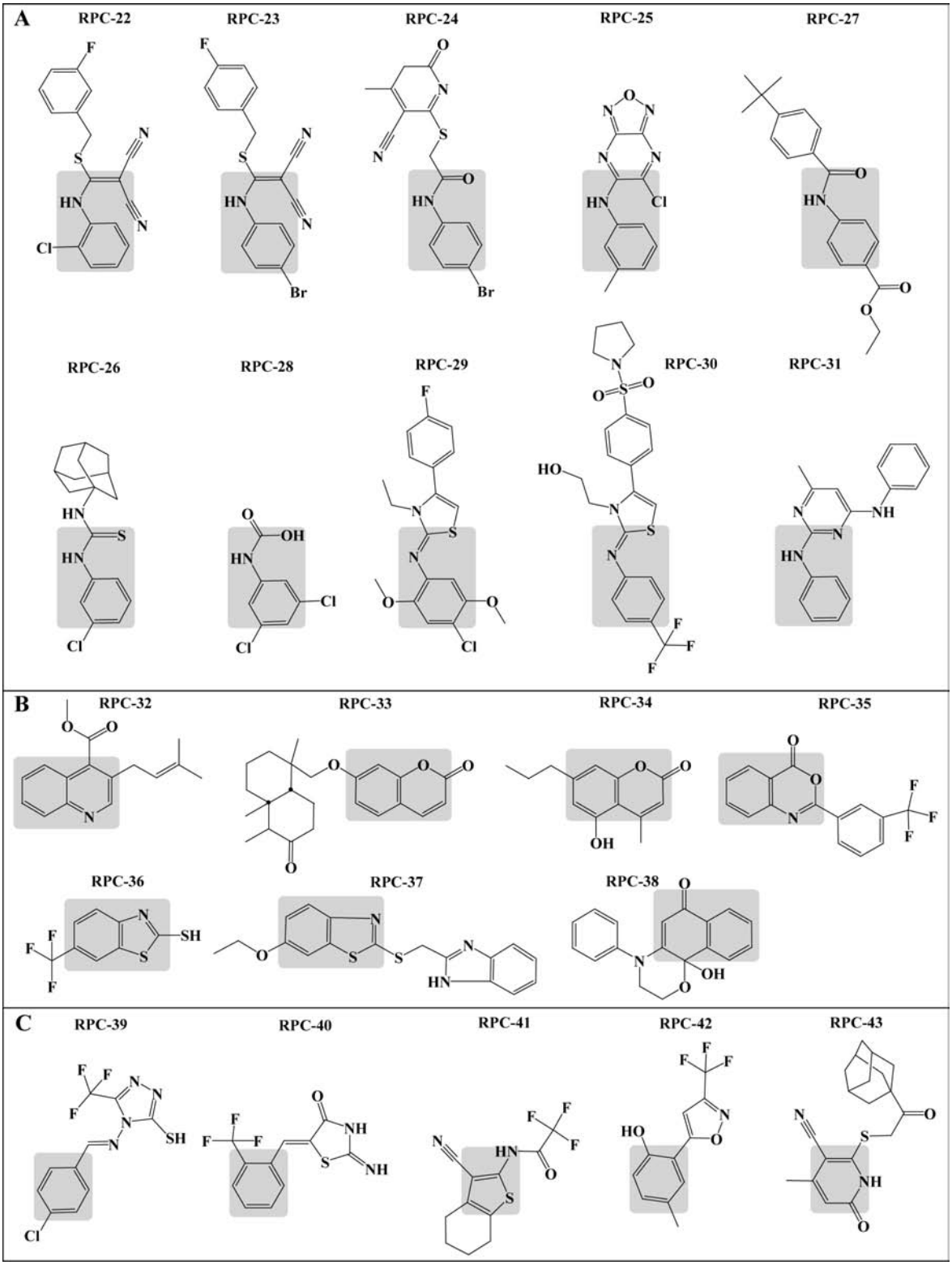

FIG. 6. Structures of all the antagonists identified in the primary screen. Chemical structures of 22 antagonists are shown. The compounds are categorized in 3 groups (**A**-**C**) of chemically related molecules by visual inspection of the structures (common substructures are highlighted in gray).

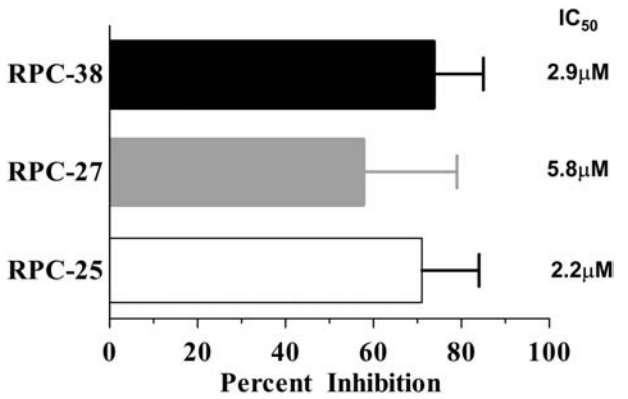

FIG. 7. Primary and secondary screening data for selected antagonists. Bar graphs show percent inhibition of cell adhesion in the presence of activating Mn^{2+}. Each bar represents the mean of duplicate wells. Cell adhesion under physiological conditions (Tris-buffered saline $[TBS]^{++}$) was considered as maximum inhibition (100%). Cell adhesion observed in the presence of buffer alone (1 mM Mn^{2+}) was assigned a value of 0% (no inhibition). The IC_{50} value for each of the compounds obtained from the secondary screen is also indicated.

ACKNOWLEDGMENTS

We thank Caroline Shamu and the rest of the ICCB staff for their support in the development and implementation of the HTS assay and Amir H. Qureshi and Constantinos J. Barth for help with the implementation of the HTS assay. This research was supported by grants DK068253 and NS053659 from the National Institutes of Health.

REFERENCES

1. Hynes RO: Integrins: bidirectional, allosteric signaling machines. *Cell* 2002;110:673-687.
2. Simon DI, Dhen Z, Seifert P, Edelman ER, Ballantyne CM, Rogers C: Decreased neointimal formation in Mac-1(–/–) mice reveals a role for inflammation in vascular repair after angioplasty. *J Clin Invest* 2000; 105:293-300.
3. Arnaout MA, Todd RF III, Dana N, Melamed J, Schlossman SF, Colten HR: Inhibition of phagocytosis of complement C3- or immunoglobulin G-coated particles and of C3bi binding by monoclonal antibodies to a monocyte-granulocyte membrane glycoprotein (Mol). *J Clin Invest* 1983;72:171-179.
4. Li R, Arnaout MA: Functional analysis of the beta 2 integrins. *Methods Mol Biol* 1999;129:105-124.
5. Rieu P, Sugimori T, Griffith DL, Arnaout MA: Solvent-accessible residues on the metal ion-dependent adhesion site face of integrin CR3 mediate its binding to the neutrophil inhibitory factor. *J Biol Chem* 1996;271:15858-15861.
6. Dunne JL, Collins RG, Beaudet AL, Ballantyne CM, Ley K: Mac-1, but not LFA-1, uses intercellular adhesion molecule-1 to mediate slow leukocyte rolling in TNF-alpha-induced inflammation. *J Immunol* 2003;171: 6105-6111.
7. Arnaout MA: Leukocyte adhesion molecules deficiency: its structural basis, pathophysiology and implications for modulating the inflammatory response. *Immunol Rev* 1990;114:145-180.
8. Horwitz AF: Integrins and health. *Sci Am* 1997;276:68-75.
9. McDowall A, Inwald D, Leitinger B, Jones A, Liesner R, Klein N, et al: A novel form of integrin dysfunction involving beta1, beta2, and beta3 integrins. *J Clin Invest* 2003;111:51-60.
10. Plow EF, Haas TA, Zhang L, Loftus J, Smith JW: Ligand binding to integrins. *J Biol Chem* 2000;275:21785-21788.
11. Tang T, Rosenkranz A, Assmann KJ, Goodman MJ, Gutierrez-Ramos JC, Carroll MC, et al: A role for Mac-1 (CDIIb/CD18) in immune complex-stimulated neutrophil function in vivo: Mac-1 deficiency abrogates sustained Fcgamma receptor-dependent neutrophil adhesion and complement-dependent proteinuria in acute glomerulonephritis. *J Exp Med* 1997;186: 1853-1863.
12. Soriano SG, Coxon A, Wang YF, Frosch MP, Lipton SA, Hickey PR, et al: Mice deficient in Mac-1 (CD11b/CD18) are less susceptible to cerebral ischemia/reperfusion injury. *Stroke* 1999;30:134-139.
13. Liu Z, Zhao M, Li N, Diaz LA, Mayadas TN: Differential roles for beta2 integrins in experimental autoimmune bullous pemphigoid. *Blood* 2006; 107:1063-1069.
14. Lange-Sperandio B, Schimpgen K, Rodenbeck B, Chavakis T, Bierhaus A, Nawroth P, et al: Distinct roles of Mac-1 and its counter-receptors in neonatal obstructive nephropathy. *Kidney Int* 2006;69:81-88.
15. Arnaout MA: Integrin structure: new twists and turns in dynamic cell adhesion. *Immunol Rev* 2002;186:125-140.
16. Jaeschke H, Farhood A, Bautista AP, Spolarics Z, Spitzer JJ, Smith CW: Functional inactivation of neutrophils with a Mac-1 (CD11b/CD18) monoclonal antibody protects against ischemia-reperfusion injury in rat liver. *Hepatology* 1993;17:915-923.
17. Wilson I, Gillinov AM, Curtis WE, DiNatale J, Burch RM, Gardner TJ, et al: Inhibition of neutrophil adherence improves postischemic ventricular performance of the neonatal heart. *Circulation* 1993;88:II372-II379.
18. Jaeschke H, Farhood A, Smith CW: Neutrophil-induced liver cell injury in endotoxin shock is a CD11b/CD18-dependent mechanism. *Am J Physiol* 1991;261:G1051-1056.
19. Rogers C, Edelman ER, Simon DI: A mAb to the beta2-leukocyte integrin Mac-1 (CD11b/CD18) reduces intimal thickening after angioplasty or stent implantation in rabbits. *Proc Natl Acad Sci USA* 1998;95: 10134-10139.
20. Burch RM, Noronha-Blob L, Bator JM, Lowe VC, Sullivan JP: Mice treated with a leumedin or antibody to Mac-1 to inhibit leukocyte sequestration survive endotoxin challenge. *J Immunol* 1993;150:3397-3403.
21. Ramamoorthy C, Sasaki SS, Su DL, Sharar SR, Harlan JM, Winn RK: CD18 adhesion blockade decreases bacterial clearance and neutrophil recruitment after intrapulmonary *E. coli*, but not after *S. aureus*. *J Leukoc Biol* 1997;61:167-172.
22. Barnard JW, Biro MG, Lo SK, Ohno S, Carozza MA, Moyle M, et al: Neutrophil inhibitory factor prevents neutrophil-dependent lung injury. *J Immunol* 1995;155:4876-4881.
23. Feng Y, Chung D, Garrard L, McEnroe G, Lim D, Scardina J, et al: Peptides derived from the complementarity-determining regions of anti-Mac-1 antibodies block intercellular adhesion molecule-1 interaction with Mac-1. *J Biol Chem* 1998;273:5625-5630.
24. Xiong JP, Li R, Essafi M, Stehle T, Arnaout MA: An isoleucine-based allosteric switch controls affinity and shape shifting in integrin CD11b A-domain. *J Biol Chem* 2000;275:38762-38767.

25. Welzenbach K, Hommel U, Weitz-Schmidt G: Small molecule inhibitors induce conformational changes in the I domain and the I-like domain of lymphocyte function-associated antigen-1: molecular insights into integrin inhibition. *J Biol Chem* 2002;277:10590-10598.
26. Bansal VS, Vaidya S, Somers EP, Kanuga M, Shevell D, Weikel R, et al: Small molecule antagonists of complement receptor type 3 block adhesion and adhesion-dependent oxidative burst in human polymorphonuclear leukocytes. *J Pharmacol Exp Ther* 2003;304:1016-1024.
27. Bjorklund M, Aitio O, Stefanidakis M, Suojanen J, Salo T, Sorsa T, et al: Stabilization of the activated alphaMbeta2 integrin by a small molecule inhibits leukocyte migration and recruitment. *Biochemistry* 2006;45: 2862-2871.
28. Cao C, Lawrence DA, Strickland DK, Zhang L: A specific role of integrin Mac-1 in accelerated macrophage efflux to the lymphatics. *Blood* 2005; 106:3234-3241.
29. Wright SD, Rao PE, Van Voorhis WC, Craigmyle LS, Iida K, Talle MA, et al: Identification of the C3bi receptor of human monocytes and macrophages by using monoclonal antibodies. *Proc Natl Acad Sci USA* 1983;80:5699-5703.
30. Li R, Haruta I, Rieu P, Sugimori T, Xiong JP, Arnaout MA: Characterization of a conformationally sensitive murine monoclonal antibody directed to the metal ion-dependent adhesion site face of integrin CD11b. *J Immunol* 2002; 168:1219-1225.
31. Dransfield I, Hogg N: Regulated expression of Mg^{2+} binding epitope on leukocyte integrin alpha subunits. *EMBO J* 1989;8:3759-3765.
32. Hogg N, Stewart MP, Scarth SL, Newton R, Shaw JM, Law SK, et al: A novel leukocyte adhesion deficiency caused by expressed but nonfunctional beta2 integrins Mac-1 and LFA-1. *J Clin Invest* 1999;103:97-106.
33. Gupta V, Lindroos A, Sugimori T, Xiong J-P, Arnaout MA: The membrane-proximal β-tail domain (βTD) regulates CD11b/CD18 activation. Submitted for publication.
34. Tan SM, Hyland RH, Al-Shamkhani A, Douglass WA, Shaw JM, Law SK: Effect of integrin beta 2 subunit truncations on LFA-1 (CD11a/CD18) and Mac-1 (CD11b/CD18) assembly, surface expression, and function. *J Immunol* 2000;165:2574-2581.
35. Lu C, Ferzly M, Takagi J, Springer TA: Epitope mapping of antibodies to the C-terminal region of the integrin beta 2 subunit reveals regions that become exposed upon receptor activation. *J Immunol* 2001;166:5629-5637.
36. Xiong JP, Stehle T, Goodman SL, Arnaout MA: New insights into the structural basis of integrin activation. *Blood* 2003;102:1155-1159.
37. Zhang JH, Chung TD, Oldenburg KR: A simple statistical parameter for use in evaluation and validation of high throughput screening assays. *J Biomol Screen* 1999;4:67-73.
38. Ortlepp S, Stephens PE, Hogg N, Figdor CG, Robinson MK: Antibodies that activate beta 2 integrins can generate different ligand binding states. *Eur J Immunol* 1995;25:637-643.
39. Annenkov A, Ortlepp S, Hogg N: The beta 2 integrin Mac-1 but not p150,95 associates with Fc gamma RIIA. *Eur J Immunol* 1996;26:207-212.
40. Beals CR, Edwards AC, Gottschalk RJ, Kuijpers TW, Staunton DE: CD18 activation epitopes induced by leukocyte activation. *J Immunol* 2001;167:6113-6122.
41. Flick MJ, Du X, Witte DP, Jirouskova M, Soloviev DA, Busuttil SJ, et al: Leukocyte engagement of fibrin(ogen) via the integrin receptor alphaMbeta2/Mac-1 is critical for host inflammatory response in vivo. *J Clin Invest* 2004;113:1596-1606.
42. Kallen J, Welzenbach K, Ramage P, Geyl D, Kriwacki R, Legge G, et al: Structural basis for LFA-1 inhibition upon lovastatin binding to the CD11a I-domain. *J Mol Biol* 1999;292:1-9.

Address reprint requests to:
Vineet Gupta, Ph.D.
Nephrology Division
Leukocyte Biology and Inflammation Program
Massachusetts General Hospital
Harvard Medical School
Charlestown, MA 02129

E-mail: vineet_gupta@hms.harvard.edu